Sánchez-Marín, JR.; Nova-Giménez, V.; Bachiller Martin, MC.; Villacampa, B.; De La Rua, A.; Kronberger, R.; Penaranda-Foix, FL.... (2019). Characterization of Nematic Liquid Crystal at Microwave Frequencies Using Split-Cylinder Resonator Method. IEEE Transactions on Microwave Theory and Techniques. 67(7):2812-2820. https://doi.org/10.1109/TMTT.2019.2916790

Characterization of Nematic Liquid Crystal at Microwave Frequencies using Split-Cylinder Resonator Method

Juan R. Sánchez, Vicente Nova, Carmen Bachiller, Belén Villacampa, Alberto de la Rua, Rainer Kronberger, Felipe Peñaranda, *Senior Member, IEEE* and Vicente E. Boria, *Fellow, IEEE*

***Abstract*—Liquid Crystal (LC) is an anisotropic liquid material which flows like a liquid, but at the same time its molecules have an orientational order like in the solid state. Thus, LC is a promising dielectric material for designing reconfigurable devices at microwave frequencies. In order to optimize the design of reconfigurable microwave devices, accurate values of the dielectric permittivity and the loss tangent of LCs are needed. However, new LCs are not well characterized at these frequencies because of its recent use for microwave applications. Therefore, the characterization in this frequency range is required for its practical use within microwave components and devices.**

In this work, a split-cylinder resonator method is used for the characterization of four different nematic LCs at two frequency points, i.e. 5 and 11 GHz. This characterization includes the extraction of their complex dielectric permittivity values at these frequencies. The employed method allows to obtain the two extreme permittivity values without applying any external electric or magnetic field to polarize the LC molecules. Two different approaches, a modal analysis method and a full-wave numerical technique have been used for determining the LC parameters obtaining similar results in both cases.

***Index Terms*—dielectric permittivity characterization, liquid crystal, microwave devices, split-cylinder resonator.**

I. Introduction

Current communication systems face the advent of spectrum saturation caused by new applications, like Internet of Things (IoT) or 5G access technology. They are defined to provide extremely high capacity, high bandwidth, and robust integrity. Thereby, radio-frequency and microwave systems must provide, among others, enhancements in terms of spectral efficiency and adaptable resource management [1]. For these reasons, the development of reconfigurable microwave devices is an area attracting research interest in recent years. Tunable behaviour can be implemented with many different methods, among them Liquid Crystal (LC) is one of the most promising materials that is used for reconfiguration of filters [2], [3], phase shifters [4], [5] and other microwave devices.

LCs are anisotropic materials whose properties are between those of crystalline solids and those of conventional liquids. LCs used in telecommunication applications are constituted by elongated rod-like organic molecules [6]. At the working temperature range, these molecules present, in general, a nematic phase, i.e. they have some orientational order but still no positional order. The long axis of the molecules has a preferred direction. This direction can change when an external low frequency electric or magnetic field is applied.

In the macroscopic scale, the direction of the molecules is represented by a vector called director ($\vec{n}$), which is parallel to the longitudinal axis of the LC molecules. The dielectric permittivity values of the nematic LCs are defined by the angle formed between the director vector and an external RF electric field $\vec{E}$. The values represented by $\varepsilon_{r\perp}$ and $\varepsilon_{r||}$ are, respectively, the permittivity values when $\vec{n}$ is perpendicular and parallel to $\vec{E}$ [7], as shown in Fig. 1. Moreover, loss tangents $tan\delta_{\perp}$ and $tan\delta_{||}$ are also defined corresponding to those directions.

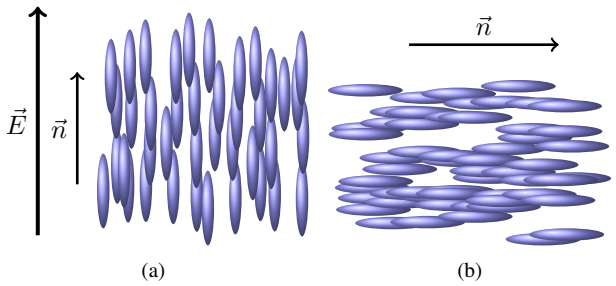

Fig. 1. Aligned LC molecules showing the director vector $\vec{n}$ and the electric field $\vec{E}$. (a) Parallel permittivity ; (b) Perpendicular permittivity

The choice of a given nematic LC for a particular application depends on a number of factors. The most determining ones are the dielectric anisotropy, the dielectric loss, and the switching voltage. The dielectric anisotropy is defined as the difference between the values of the parallel and perpendicular permittivities, $\Delta\varepsilon_r = \varepsilon_{r|||} - \varepsilon_{r\perp}$. This value

This work was supported by the Generalitat Valenciana research project PROMETEOII/2015/005, by the Ministerio de Educación, Cultura y Deporte (Spain) under the Fellowship Program for Training University Professors FPU14/00150, by Ministerio de Economía y Competitividad (Spain) under R&D projects TEC2016-75934-C4-R-1, by Gobierno de Aragon-FEDER-Fondo Social Europeo 2017-2019 under reference E14-7R.

J. R. Sánchez, V. Nova, C. Bachiller, and V. E. Boria are with Instituto de Telecomunicaciones y Aplicaciones Multimedia. Universitat Politècnica de València. Camino de Vera, s/n, 46021 Valencia, Spain. e-mail: juasncm1@iteam.upv.es vinogi@teleco.upv.es, mabacmar@dcom.upv.es, vboria@dcom.upv.es.

B. Villacampa is with Departamento de Fisica de la Materia Condensada. Universidad de Zaragoza. C/ Pedro Cerbuna 12, 50009 Zaragoza, Spain. email: bvillaca@unizar.es.

A. Rua and R. Kronberger are with High Frequency Laboratory. Cologne University of Applied Sciences. Betzdorfer Str. 2, D-50679 Koeln, Germany. email: alberto.de_la_rua_lope@th-koeln.de, rainer.kronberger@th-koeln.de.

F. Peñaranda is with ITACA Research Institute. Universitat Politècnica de València. Camino de Vera, s/n, 46021 Valencia, Spain. email: fpenaran@dcom.upv.es.

directly determines the tunability/control range of an LC-based microwave device.

Thus, it is important to determine the dielectric anisotropy at microwave frequencies. Different methods based on transmission lines have been used to characterize the dielectric properties of LCs at millimeter-wave and microwave frequencies. In [8], a broadband coaxial line is used, in [9] the measurement is done using a rectangular waveguide and [10] uses a covered microstrip. These methods can measure the dielectric properties of the LCs in a wide frequency range, but sometimes they are not accurate enough.

Other methods can be used to determine the anisotropy of LCs at microwave frequencies, such as the resonator-based methods, which have higher sensitivity and better accuracy [11]. Such these methods can determine the dielectric properties of materials at single frequency points. In [12] a rectangular cavity perturbation method is proposed for characterizing a polytetrafluoroethylene (PTFE) tube filled with LC, and in [13], [14] a split-post dielectric resonator technique is used for characterizing LC mixtures in silicon cells. Resonator methods in planar structures as in [15], which uses a patch resonator, can be used too.

However, the previously mentioned methods need an electric or magnetic field to align the molecules in the two directions (perpendicular and parallel). The use of external fields for the alignment has proved to give excellent results, but it requires a decoupled electric structure for the electric field alignment, or a laboratory setup for the magnetic field one [16]. Alternatively, an accurate and non-destructive characterization method is proposed in this paper, and it is used for measuring four different nematic LCs mixtures at two different frequency points, i.e. 5 and 11 GHz. This method allows to measure the two extreme values of permittivity and loss tangent without applying any external electric or magnetic field. This measuring procedure and its results are explained in detail and discussed in the following sections.

II. Split-cylinder resonator method

Resonator methods are widely used for material characterization due to their high accuracy and sensitivity [17]. Among them, resonators implemented on dielectric substrate must be redesigned for each measured material and frequency. However, cavity resonator methods, as the split-cylinder one, can measure all the samples at one frequency without changing the housing resonator [18], [19].

The split-cylinder resonator consists on two cylindrical halves, where a sample is placed in the gap between the two sections, as shown in Fig. 2. Two coupling loops are used to feed the cavity and excite the TE modes inside the resonator. As can be seen in Fig. 2 (c) and (d), these loops also define the electromagnetic field direction.

The dimensions of the cavity, the thickness of the sample and the resonance frequency are the parameters needed to calculate the dielectric properties of the materials (relative permittivity and loss tangent). The dimensions of the cylinder, i.e. the radius and the length, must be chosen considering the resonance frequency and the electromagnetic field distribution of the empty cavity resonator.

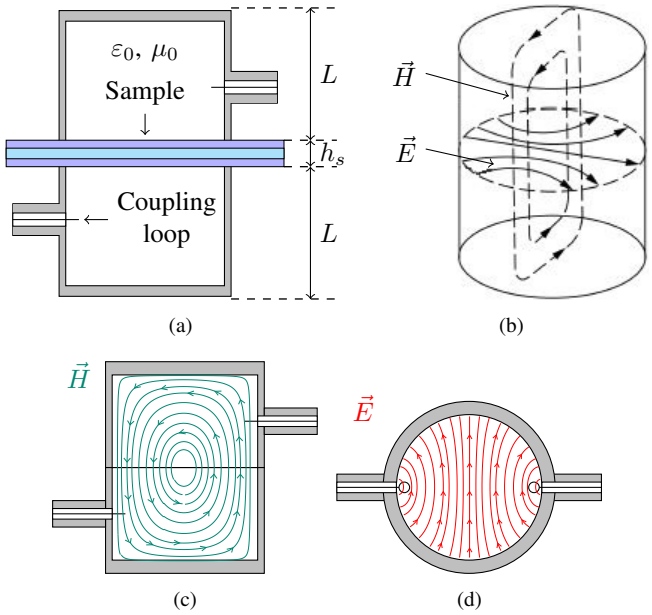

Fig. 2. Split-cylinder resonator. (a) Front view. In gray the brass of the cylinder, in blue the sample (glasses (h_g) in dark blue and liquid crystal (h_{LC}) in light blue) and in white the air. (b) 3D view with $\vec{E}$ and $\vec{H}$ fields. (c) Front view with $\vec{H}$ field. (d) Top view with $\vec{E}$ field.

In order to calculate these dimensions, the general equation of resonance frequencies of TE_{mnp} modes within a cylindrical resonator is used:

$$(f_r)^{TE}_{mnp} = \frac{1}{2\pi\sqrt{\mu\varepsilon}}\sqrt{\left(\frac{\chi'_{mn}}{a}\right)^2 + \left(\frac{p\pi}{2L}\right)^2} \qquad (1)$$

where:

- f_r is the resonance frequency.
- χ_{mn} is the m-th root of first-order derivative of Bessel function of n-th order.
- a is the radius of the cavity.
- L is the half-length of the cavity.
- μ is the permeability inside the cavity.
- ε is the permittivity inside the cavity.

The criterion to choose one mode is based on the field distribution inside the cavity and the clear spectral separation. Traditionally, TE_{011} mode is used by Kent and Janezic [18], [19]. Nevertheless, in the case of the characterization of an anisotropic material, as the LC used in this work, the transverse electric field must present a linear polarization. The field distribution that better fits this requirement is the one of TE_{11p} modes, since it has quite straight field lines in the center of the cavity [20] as shown in Fig. 2(b). In our case, the TE_{111} mode is finally employed since the electric field reaches a maximum in the center of the cavity where the sample is placed. In addition, it has the advantage of being the fundamental mode, i.e. the one resonating at the lowest frequency, and presents a high quality factor (Q).

Two different cylinders have been designed to yield the resonance frequencies of the TE_{111} mode at 5 GHz and 11 GHz, respectively. The resultant dimensions are detailed in Table I.

TABLE I
DIMENSIONS OF THE SPLIT-CYLINDER RESONATORS.

Parameter	$f_{u0} = 5$ GHz	$f_{u0} = 11$ GHz
a	20.00 mm	10.00 mm
L	32.00 mm	11.20 mm

III. MEASUREMENT PROCEDURE

The split-cylinder resonator method is based on the fact that the resonance frequency and Q-factor are mostly determined by the permittivity and permeability inside the cavity. When part of the electromagnetic boundary condition is changed by introducing a sample, the resonance frequency and Q-factor will also change as shown in Fig. 3. The resonance frequency (f_{u0}) of the empty cylinder will move to a lower frequency (f_{us}) when the sample is placed, and the value of the quality factor (Q_{u0}) will be reduced (Q_{us}).

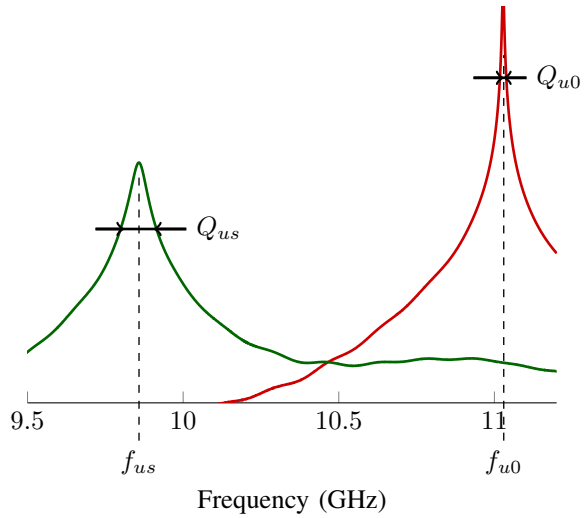

Fig. 3. Resonance frequency and Q factor for the resonator without (f_{u0}) and with (f_{us}) sample.

With these two measurements, with and without sample, the permittivity value and the loss tangent of a single material can be determined by the Kent method [18]. However, the LC must be confined in a sealed cell, i.e. a "sandwich" formed by two glasses and the LC between them, as explained in Section IV. Since the LC cell is a non uniform material, formed by two glasses and one LC layer, all the thicknesses of this cell (glasses and LC) and the dielectric properties of the glasses must be characterized. Hereby, the measurements process is carried out in two steps.

First, the thickness of each glass is measured and then, their permittivity and loss tangent are characterized by the Kent method, detailed in [18]. Next, the thickness of the LC is measured, so the only unknown is the LC complex permittivity. Finally, the whole LC sealed cells are placed in the split-resonator and their frequency response is measured. With all measurements, the electromagnetic properties of LC can be determined following two different methods.

A. Numerical method

Once the glass permittivity and dimensions of the LC cells and the measurement set-up (split-cylinder resonator and connectors) are known, an electrical model is simulated in a numerical electromagnetic simulation software, CST[1]. The fields inside the structure are iteratively simulated as a function of the complex permitivitty of the sample material. This process ends when the simulated resonance frequency and quality factor are as similar as possible to the measured ones. The complex permittivity value of the LC is adjusted by using an hybridization of different optimization algorithms. The process starts assuming a $\tan\delta = 0$, and the datasheet permittivity values of the LC mixtures at optical frequencies. Next, a Nelder Mead Simplex Algorithm is applied in order to optimize the $\tan\delta$ and ε values, until the Q-factor and resonance frequency errors are below 5 and 1 MHz, respectively. Then, the Trust Region Framework method is applied with an initial searching area radius of 0.2 which means that the algorithm looks for a minimum in a restricted area. When the error of the Q-factor is below 0.5 and the resonance frequency error is below 1 MHz, the optimization algorithm is finally changed to a Quasi Newton method. The entire process comprises circa 70 evaluations, which takes about 5 hours.

B. Modal method

In order to characterize the LC, the method in [21], [22] is also employed. It implements a full-wave circuit analysis of the structure (split-cylinder with an LC cell), based on a modal analysis method. Accordingly, it is much more accurate and requires a lower computational cost than a numerical method (based on FDTD or FEM) like the previous one (Section III.A), but requires the resolution of the full-wave circuit for each particular structure.

In this method , the whole structure is divided into simpler small structures or networks that can be solved in an easier way, i.e. it is segmented into canonical circuital elements. Then, the small structures can be joined in order to give the general solution of the whole structure. In the case under study, the split cavity with the LC cell is segmented into 8 small structures, as shown in Fig. 4 (a), where some surfaces have been defined as ports, as can be seen in Fig. 4 (b). In this configuration, the upper and lower zones model the air filled resonator sections (each one is a 3-port network), the second and the fourth zones model the glass of the cell (two 3-port networks for each one), and the central region models the LC sample (two 3-port networks).

Once the structure has been split, each circuit is electromagnetically characterized by its Generalized Admittance Matrix (GAM) which is computed by using the mode matching method. With this modal method, the electromagnetic fields of each port network are approximated by the series expansion [23] of equation (2). Since the proposed method is a full-wave circuit analysis, every possible electromagnetic modes inside the structure has been taken into account, i.e. TE_{mn} and TM_{mn}.

[1]CST Studio Suite, v2017

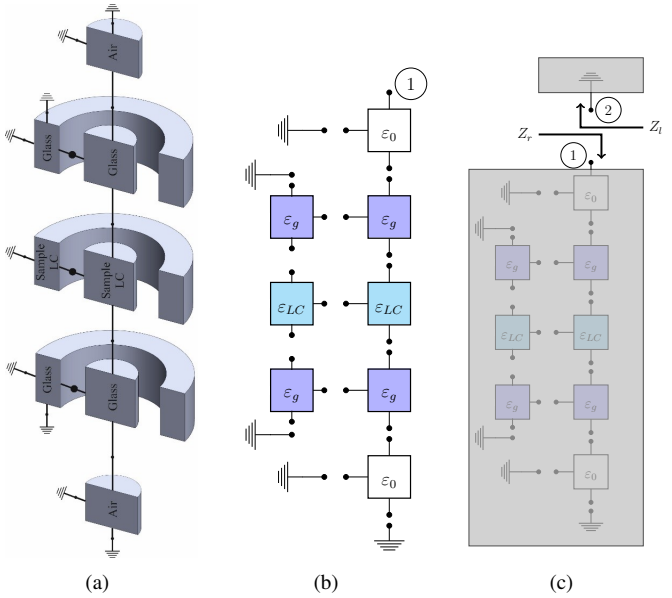

Fig. 4. Circuital model of the split-cylinder resonator and the liquid crystal cell segmented into 8 simple circuits. (a) Graphic representation. (b) Schematic representation. (c) Schematic representation forcing the resonance condition.

$$\vec{E}_{port} = \sum_n e_n \cdot \vec{E_n} \quad ; \quad \vec{H}_{port} = \sum_n h_n \cdot \vec{H_n} \tag{2}$$

where:

- $\vec{E}_{port}$ and $\vec{H}_{port}$ are the electric and magnetic fields in the port surface.
- e_n and h_n are the amplitudes of each base function.
- $\vec{E_n}$ and $\vec{H_n}$ are the base functions for the electric and magnetic fields.

According to equation (2), the relation between electric and magnetic fields can be established by the general GAM matrix for an N-port network represented in equation (3).

$$\mathbf{h} = \begin{pmatrix} h_1 \\ h_2 \\ \dots \\ h_N \end{pmatrix} = \begin{pmatrix} \mathbf{Y_{11}} & \mathbf{Y_{12}} & \dots & \mathbf{Y_{1N}} \\ \mathbf{Y_{21}} & \mathbf{Y_{22}} & \dots & \mathbf{Y_{2N}} \\ \dots & \dots & \dots & \dots \\ \mathbf{Y_{N1}} & \mathbf{Y_{N2}} & \dots & \mathbf{Y_{NN}} \end{pmatrix} \begin{pmatrix} e_1 \\ e_2 \\ \dots \\ e_N \end{pmatrix} = \mathbf{Y} \cdot \mathbf{e} \tag{3}$$

In the GAM matrix, each h_n and e_n element is a vector with the coefficient of the series expansion shown in equation (2). Consequently, each element $\mathbf{Y_{ij}}$ is not a scalar value but a matrix. Thus, any $\mathbf{Y_{ij}}$ element of each network can be calculated by forcing the boundary conditions of the particular network and a short circuit condition in the other ports for every considered base function.

Once every GAM network is calculated, the networks are connected to each other enforcing the boundary conditions. A recursive method by pairs is used to obtain the GAM of the whole structure [21]. This new GAM is obtained for only one port (port 1 of Fig. 4 (c)). This port is then connected to ground (port 2 of Fig. 4 (c)) to force the resonance condition, which leads to solve equation (4).

$$|\det\left(\mathbf{Z_r}(dim, \varepsilon, \mu, f) + \mathbf{Z_l}(dim, \varepsilon, \mu, f)\right)| = 0 \tag{4}$$

where:

- $\mathbf{Z_r}$ and $\mathbf{Z_l}$ are the Generalized Impedance Matrices, defined as the inverse of the GAM, of each 1-port network (see Fig. 4 (c)).
- dim contains the dimensions of the resonator and LC cells.
- ε is the LC permittivity.
- μ is the LC permeability.
- f is the resonance frequency when the LC cell is placed in the resoantor.

As can be seen in equation (4), every GAM network is a function of the dimensions of the structure, its electromagnetic properties (permeability and permittivity) and frequency. All these variables are known except the LC complex permittivity, which can be obtained by forcing this resonance condition [23].

Both methods, the numerical and the modal, need a calibration of the split-cylinder resonator. This calibration consists in modelling the empty resonant cavity (without dielectric material) in order to adjust the values of the feeding network, the real dimensions, characteristics and configuration of the resonator (radius, height, and conductivity of the brass walls).

This is the starting point of the data analysis of each considered LC samples, as it is shown in the next section.

IV. Liquid crystal samples

In order to perform the practical estimation of the two relative permittivities ($\varepsilon_{r\perp}$ and $\varepsilon_{r||}$) with the split-cylinder resonator method, the samples of liquid crystal must be previously treated. LC must be contained in a cell composed of two support glasses separated with spacers and glued. Each glass has a thickness of 400 μm $\pm$ 10 μm and they are separated around 0.150 mm. The process for the construction of the cells is described next:

Glass cleaning. The glass should be as clean as possible, because even microscopic particles could damage the homogeneity of the alignment layer, affecting the separation between the glasses of the cell. Hence, a meticulous cleaning process is done in two stages. In the first one, the fat and larger particles are removed. Next, an ultrasonic cleaning process is conducted.

After this, the glasses are dried and stored in hermetic containers to avoid possible contamination. Immediately before the next process (alignment surface), the glass substrates are subjected to a UV-ozone-cleaning procedure.

Alignment surface. To characterize the value of the dielectric anisotropy of the LC, its molecules must present a well defined orientation. For that, an alignment surface is created on one side of each glass of the cell. The creation of this alignment by anchoring surface is carried out in three main steps: the deposition of polyimide, the curing of this polymer, and the realization of the microscopic grooves.

The deposition of the polyimide is done with a spin coating mechanism to get a uniform surface of approximately 100 nm.

This thickness is an average value obtained with a contact profilometer (Dektak XT).

After deposition, the samples are cured to get the polymerization of the polyimide, thus, the material is hardened.

Finally, the samples are ready to make the microgrooves that will determine the orientation of the LC molecules. To do this, a rubbing process on a natural silk velvet, which leaves no residue, is followed. It is very important to perform rubbing in a unique way, since this will determine the initial orientation of the molecules. To achieve a homogeneous alignment direction, the velvet is fastened together to a straight tray on which one of the faces of the glass can rest and move in a specific direction.

Cells assembly. To form the LC cell, four Mylar separators are adhered near the corners of the glass with optic glue. This action allows to separate homogeneously the two glasses that make up the cell. Another glass is superimposed over the separators. Both glasses have the same alignment layer direction. A separation between both glasses acting as a "bed" has to be included for the filling process, as shown in Fig. 5. Next, the cell is consolidated (applying pressure) and cured using an ultraviolet light oven.

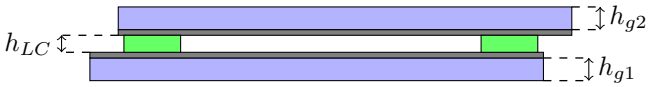

Fig. 5. Layout of an empty liquid crystal cell. In blue the glasses, in gray the polyimide surfaces, in green the spacers and in white the gap for the liquid crystal.

As mentioned before, the thickness of the materials used in the characterization presents a great relevance in the obtained results. For that reason, the thickness of the glasses of each cell has been measured in 8 different points and at two different times: before and after assembling the cells. A micrometer screw (Mitutoyo) with an uncertainty of $\pm$ 2 μm has been used for the measurement. For each glass of the four cells, the average thickness is detailed in Table II.

The glass permittivity and loss tangent were measured at the two selected frequencies using the Kent method [18] for different glasses and positions, to ensure the isotropy of the material. The results are shown in Table III. Since the error margin of the glass measurements is below 0.2% and 0.001% in terms of complex permittivity and loss tangent respectively, the effect in the final LC results is negligible.

TABLE II
AVERAGE THICKNESS OF THE GLASSES (h_{gi}) OF THE FOUR LC CELLS.

Cell	Glass 1 (μm)	Glass 2 (μm)
TH1	410 ± 2	410 ± 2
TH2	404 ± 2	410 ± 2
TH3	410 ± 2	410 ± 2
TH4	409 ± 2	409 ± 2

The thickness of the gap between the two glasses of each cell has been measured by using a spectrophotometer (Cary 5000 UV-Vis-NIR from Agilent). The measurement of the thickness has been made taking advantage of the Fabry-Perot resonance that occurs in the glass-air-glass interface of the LC cell.

TABLE III
AVERAGE MEASUREMENT OF THE EM PROPERTIES OF THE GLASS.

Parameter	Resonator (5 GHz)	Resonator (11 GHz)
$f_{us-glass}$ (GHz)	$4.7708 \pm 3.2 \times 10^{-6}$	$9.841 \pm 3.5 \times 10^{-4}$
Q_{glass}	673.1 ± 3.7	231.69 ± 1.2
ε_r	$7.2102 \pm 3 \times 10^{-4}$	$7.0101 \pm 2 \times 10^{-5}$
$\tan\delta$	$0.0155 \pm 4 \times 10^{-9}$	$0.0171 \pm 4 \times 10^{-9}$

The optical transmission spectrum of each empty cell, recorded as a function of the wavelength, shows a series of maxima and minima due to the interference phenomena originated by multiple reflections at the glass-air-glass interfaces. The frequency difference between consecutive maxima is related to the air gap thickness (h_{LC}), according to the expression (5).

$$\Delta f = \frac{c}{2h_{LC}n} \tag{5}$$

where:

- Δf is the frequency space between two consecutive maximums.
- c is the speed light in the vacuum. c = 299792458 m/s.
- h_{LC} is the separation between glasses.
- n is the refraction index of the medium (in this case the air: n = 1).

The smaller the spacing, the greater the frequency separation will be. Thus, it will be easier to distinguish the maxima or minima. For this reason, this method is used for measuring very small values of thickness (thin samples).

Taking into account this phenomenon, a relationship between the separation of the glasses h_{LC} and the number m of minima (or maxima) in a bandwidth can be obtained. This bandwidth is defined by two non-consecutive maxima (or minima) located at the wavelengths λ_1 and λ_2.

$$h_{LC} = \frac{m\lambda_1\lambda_2}{2n|\lambda_2 - \lambda_1|} \tag{6}$$

To confirm the results obtained by this interferometric method, the total thickness of the cells was also measured with the micrometer screw over the spacers (to prevent warping of the glasses), thereby subtracting the thickness of the glasses of Table II, the gap h_{LC} between the glasses can be calculated. Both measurement results are shown and compared in Table IV.

TABLE IV
AVERAGE THICKNESS OF THE GAP OF THE LC CELLS (h_{LC}).

Cell	Interferometric measurement (μm)	Micrometer screw measurement (μm)
TH1	156	155 ± 9
TH2	151	150 ± 8
TH3	153	151 ± 3
TH4	146	144 ± 3

After obtaining the measurements of both the glasses and the gap separation, the LC cells can be filled in. They are filled by depositing the material on the "bed", and the LC, by capillarity, extending the material within the whole cell, as

shown in Fig. 6. Then, the cells are sealed with optical glue to prevent the emptying during the measurement process.

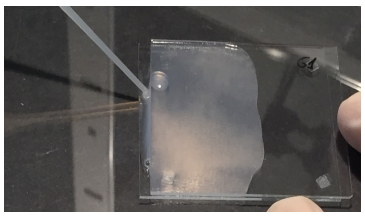

Fig. 6. Filling process of an LC cell by capillarity.

One of the great advantages of using LC cells formed by transparent glasses is the possibility to check the correct alignment of the molecules. The asymmetry of the LC molecules and their orientation, parallel to the polyimide rubbing, explain the birefringence property of this material. When two linear polarizers are placed orthogonally (crossed polarizers) over a source of white light with an isotropic medium in between, light transmission is blocked. This happens because the polarization induced by the first polarizer is essentially maintained through the isotropic medium and so, it is totally filtered by the orthogonal second polarizer. This is what happens in the dark zones of Fig. 7 (b), where air fills the gap between the polarizers.

If a LC cell (with its axis rotated 45° with respect to the linear polarizers) is introduced between the two crossed polarizers, the light with linear polarization that goes through the first polarizer can be decomposed in the axes of the LC molecules into two orthogonal polarizations (Fig. 7 (a)) that, crossing the same medium, present different refractive indexes (different permittivity). This implies that the components travel at different speeds and, therefore, a phase shift between them is introduced. The result is a change in the polarization of light from linear to elliptical, therefore, when the light crosses the material and reaches the second polarizer, part of it passes through. This effect can be clearly seen in Fig. 7 (b).

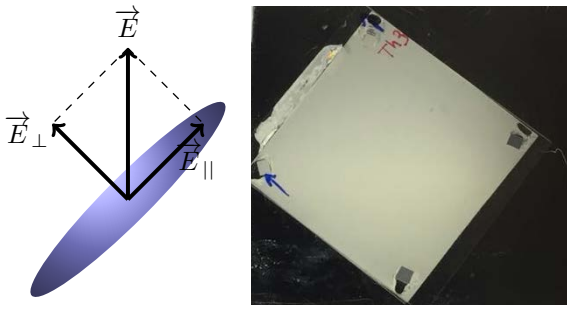

(a) (b)

Fig. 7. (a) Electric field decomposed in the axes of an LC molecule. (b) LC cell rotated 45° with respect to the crossed polarizers.

This alignment procedure enables to measure the two extreme permittivity values without applying any external electric or magnetic field. For that, taking into account the field distribution of the mode TE_{111} shown in Fig. 2(d), the cell is placed into the resonator with the molecules aligned in the same direction of the E-field, i.e. parallel to the major field distribution to measure ε_{rpos1}. Then, the cell is placed in the opposite direction (turned 90^o perpendicular to the major field distribution) to measure ε_{rpos2}, as can be seen in Fig. 8(a) and 8(b), respectively.

Since the E-field vector direction is not ideal for the TE_{111} mode, the ε_{rpos1} and ε_{rpos2} do not correspond to $\varepsilon_{r||}$ and $\varepsilon_{r\perp}$, so the field distribution of the cell should be considered in order to extract the precise values as stated in eq. (7).

$$\begin{aligned} \varepsilon_{rpos1} \iint |\vec{E}| dS &= \varepsilon_{r\perp} \iint E_\perp dS + \varepsilon_{r||} \iint E_{||} dS \\ \varepsilon_{rpos2} \iint |\vec{E}| dS &= \varepsilon_{r||} \iint E_\perp dS + \varepsilon_{r\perp} \iint E_{||} dS \end{aligned} \tag{7}$$

where:

- ε_{rpos1} and ε_{rpos2} are the extracted complex permittivities with the cells in position 1 and 2 respectively, assuming an ideal (lineal polarization) E field .
- $|\vec{E}|$ is the module of the electric field calculated in each point of the cell, with the real polarization shown in Fig. 2 (d).
- $E_{||}$ is the component of the electric field in the parallel direction, see Fig. 8 (c).
- $E_\perp$ is the component of the electric field in the normal direction, see Fig. 8 (c).

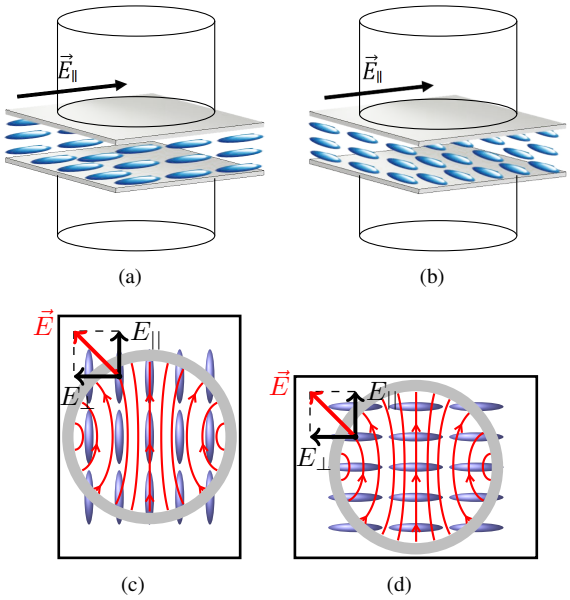

(a) (b) (c) (d)

Fig. 8. (a) Placement of sample in Pos1. (b) Placement of sample in Pos2. (c) E-field and LC molecules in Pos1. (d) E-field and LC molecules in Pos2.

Although the actual cavity does not have a perfect electric wall when the sample is placed, the work in [19] validates the assumption of considering that fringing fields vanish outside the resonator.

V. Results

The set-up used for performing the measurements is shown in Fig. 9. Four cells with different nematic LCs have been prepared and measured: QYPD036 (Q036, in cell TH1) , QYPD142 (Q142, in cell TH2) , and QYPD193 (Q193, in cell

TH3) from Qingdao QY Liquid Crystal Co and GT3-23002 (GT3, in cell TH4) from Merck. The measurements have been carried out at two different frequencies (5 GHz and 11 GHz) at room temperature (25°C).

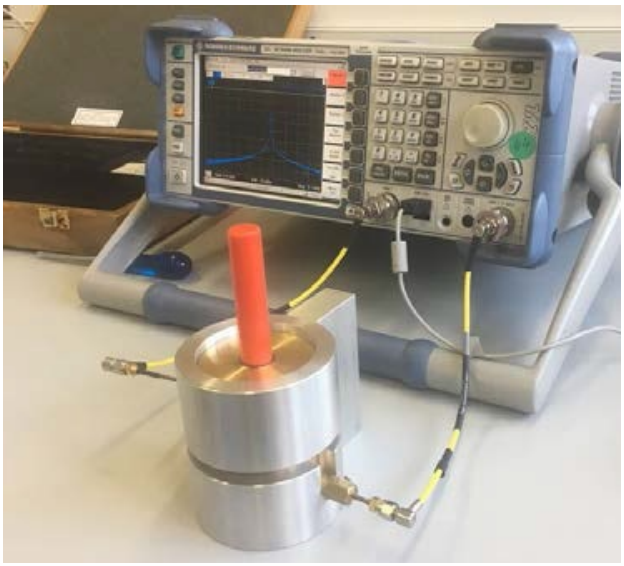

Fig. 9. Measurement setup: VNA and split-cylinder resonator.

For each cell TH$_i$, the resonance frequency and the Q factor for positions 1 and 2 have been measured several times, see Tables V and VIII. With these values and following the two methods explained above, the complex dielectric permittivity values are obtained. Then, the transformation explained in (7) is applied to obtain the parallel and perpendicular dielectric permittivity and the loss tangent is calculated.

There are many error sources that affect the extraction of the complex permittivity: the features of the cylinder (dimensions a and L, conductivity, feeding loops), the measured EM response (f_{us} and Q_{us}), the thickness of the glasses (h_{g1} and h_{g2}) and the thickness of liquid crystal (h_{LC}). The impact of the cylinder dimensions (a, L, conductivity, and feeding loops) is calibrated and compensated with a first measurement of the empty cylinder. However, the tolerance in the measurement of the other parameters is translated into a set of uncertainties (σ_i) and their error contribution to the complex permittivity results is quantified ($\frac{\partial \varepsilon}{\partial i}$). Then, if the error contribution of these parameters is independent and known, the total uncertainty of the complex dielectric permittivity can be expressed as the quadrature sum [24] described in equation (8). Finally, the complex permittivity error can be easily propagated to obtain the loss tangent uncertainty.

$$\sigma_\varepsilon = \left(\left|\frac{\partial \varepsilon}{\partial f}\right|^2 \sigma_f^2 + \left|\frac{\partial \varepsilon}{\partial Q}\right|^2 \sigma_Q^2 + \left|\frac{\partial \varepsilon}{\partial h_{g1}}\right|^2 \sigma_{h_{g1}}^2 + \right. \\ \left. + \left|\frac{\partial \varepsilon}{\partial h_{g2}}\right|^2 \sigma_{h_{g2}}^2 + \left|\frac{\partial \varepsilon}{\partial h_{LC}}\right|^2 \sigma_{h_{LC}}^2 \right)^{\frac{1}{2}} \tag{8}$$

The results corresponding to 5 GHz are presented in Tables VI and VII for the modal and numerical methods, respectively. Moreover, resulting values for 11 GHz are presented in Tables IX and X for the modal and numerical methods, respectively. Comparing the values of permittivity and loss tangent obtained with both methods, they are in very good agreement, so it can be said that the results are consistent. The highest value of anisotropy ($\Delta\varepsilon_r$) for the Qingdao LCs family, is 0.81 at 5 GHz (QYPD193) and 0.98 at 11 GHz (QYPD036). The highest values of the loss tangents are also recorded for these two materials. Therefore, choosing an LC for designing a reconfigurable microwave device must be a trade-off between the dielectric anisotropy and the related loss, depending on the required specifications.

TABLE V
LC MEASUREMENT AT 5 GHZ

LC	$f_{us-pos1}$ (MHz)	Q_{pos1}	$f_{us-pos2}$ (MHz)	Q_{pos2}
Q036	4528±0.13	281.61±1.5	4533±0.28	245.3±0.51
Q142	4536±0.07	298.94±1.49	4540±0.07	255.6±0.07
Q193	4530±0.18	292.99±2.11	4537±0.09	238.94±0.09
GT3	4537±0.017	308.51±3.76	4543±0.09	286.05±0.09

TABLE VI
RESULTS AT 5 GHZ USING MODAL METHOD

LC	$\varepsilon_{r\parallel}$	$tan\delta_{\parallel} \times 1000$	$\varepsilon_{r\perp}$	$tan\delta_{\perp} \times 1000$
Q036	3.08±0.19	17.06±2.08	2.28±0.15	75.45±7.89
Q142	2.72±0.17	7.95±1.09	2.27±0.16	58.51±7.20
Q193	3.03±0.19	7.14±0.97	2.22±0.15	91.90±7.55
GT3	2.59±0.15	5.13±1.79	1.94±0.14	39.33±10.90

TABLE VII
RESULTS AT 5 GHZ USING NUMERICAL METHOD

LC	$\varepsilon_{r\parallel}$	$tan\delta_{\parallel} \times 1000$	$\varepsilon_{r\perp}$	$tan\delta_{\perp} \times 1000$
Q036	3.11±0.22	17.01±2.67	2.29±0.19	75.61±9.45
Q142	2.74±0.15	8.73±2.03	2.26±0.13	65.97±6.70
Q193	3.07±0.10	6.64±0.70	2.22±0.13	94.82±14.51
GT3	2.63±0.16	4.81±2.27	1.97±0.17	39.14±11.81

TABLE VIII
LC MEASUREMENT AT 11 GHZ

LC	$f_{us-pos1}$ (MHz)	Q_{pos1}	$f_{us-pos2}$ (MHz)	Q_{pos2}
Q036	8716±0.58	127.54±1.02	8754±0.42	108.75±0.58
Q142	8742±0.55	129.24±1.02	8767±0.96	115.78±0.17
Q193	8725±0.35	128.15±0.2	8757±0.16	106.19±0.18
GT3	8735±0.61	133.02±1.26	8767±0.32	124.82±1.59

TABLE IX
RESULTS AT 11 GHZ USING MODAL METHOD

LC	$\varepsilon_{r\parallel}$	$tan\delta_{\parallel} \times 1000$	$\varepsilon_{r\perp}$	$tan\delta_{\perp} \times 1000$
Q036	3.22±0.19	3.95±0.67	2.24±0.15	57.51±6.80
Q142	3.05±0.18	5.80±1.06	2.36±0.16	40.88±4.92
Q193	3.26±0.20	1.97±0.11	2.40±0.17	63.31±4.40
GT3	3.25±0.21	2.50±0.83	2.35±0.17	22.05±3.81

VI. CONCLUSION

In this work, the split-cylinder resonator method has been used for the characterization of LCs at microwave frequencies.

TABLE X
RESULTS AT 11 GHZ USING NUMERICAL METHOD

LC	$\varepsilon_{r\|\|}$	$tan\delta_{\|\|} \times 1000$	$\varepsilon_{r\perp}$	$tan\delta_{\perp} \times 1000$
Q036	3.22±0.20	3.47±0.80	2.23±0.19	71.38±18.57
Q142	3.09±0.21	6.63±1.76	2.33±0.15	43.05±3.77
Q193	3.26±0.16	3.58±0.54	2.34±0.17	60.43±4.75
GT3	3.32±0.20	3.70±1.00	2.32±0.0.16	19.92±5.20

The method is based on the measurement of the resonance frequency and quality factor of the two states of the LC molecules. To achieve these two states, no electric or magnetic fields are needed, instead the cell must be turned 90° inside the cavity. The dielectric properties (permittivity and loss tangent) of four different LC samples, GT3-23002 from Merck and QYPD193, QYPD142, and QYPD036 from Qingdao QY Liquid Crystal Co, have been obtained. The highest values of the dielectric anisotropy are presented for the samples QYPD036 and QYPD193, together with the highest values of the corresponding loss tangent parameters. Furthermore, it is observed for all the LCs that the loss tangent decreases and the dielectric anisotropy increases at higher frequencies. This must be taken into account in the development of reconfigurable microwave devices.

REFERENCES

[1] S. Borkar and H. Pande, "Application of 5G next generation network to internet of things," in *2016 Int. Conf. on Internet of Things and Applications (IOTA)*, Jan 2016, pp. 443–447.

[2] M. Yazdanpanahi and D. Mirshekar-Syahkal, "Millimeter-wave liquid-crystal-based tunable bandpass filter," in *2012 IEEE Radio and Wireless Symp.*, Jan 2012, pp. 139–142.

[3] M. Jost, C. Weickhmann, T. Franke, A. E. Prasetiadi, W. Hu, M. Nickel, O. H. Karabey, and R. Jakoby, "Tuneable hollow waveguide devices for space applications based on liquid crystal," in *2015 SBMO/IEEE MTT-S Int. Microw. and Optoelectronics Conf. (IMOC)*, Nov 2015, pp. 1–5.

[4] S. Strunck, O. H. Karabey, C. Weickhmann, A. Gaebler, and R. Jakoby, "Continuously tunable phase shifters for phased arrays based on liquid crystal technology," in *2013 IEEE Int. Symp. on Phased Array Systems and Technol.*, Oct 2013, pp. 82–88.

[5] K. Wang and K. Wu, "Liquid crystal enabled substrate integrated waveguide variable phase shifter for millimeter-wave application at 60 GHz and beyond," in *2015 IEEE MTT-S Int. Microw. Symp.*, May 2015, pp. 1–4.

[6] D. Yang and S. Wu, *Fundamentals of Liquid Crystal Devices*. West Sussex, England: John Wiley & Sons, Ltd., 2006.

[7] O. H. Karabey, *Electronic Beam Steering and Polarization Agile Planar Antennas in Liquid Crystal Technology (Springer Theses)*. Springer, 2013.

[8] S. Mueller, A. Penirschke, C. Damm, P. Scheele, M. Wittek, C. Weil, and R. Jakoby, "Broad-band microwave characterization of liquid crystals using a temperature-controlled coaxial transmission line," *IEEE Trans. Microw. Theory Techn.*, vol. 53, no. 6, pp. 1937–1945, June 2005.

[9] S. Mueller, M. Koeberle, F. Goelden, A. Penirschke, A. Gaebler, A. Lapanik, W. Haase, and R. Jakoby, "W-band characterization of anisotropic liquid crystals at room temperature," in *2008 38th Eur. Microw. Conf.*, Oct 2008, pp. 119–122.

[10] S. Bulja, D. Mirshekar-Syahkal, R. James, S. E. Day, and F. A. Fernandez, "Measurement of dielectric properties of nematic liquid crystals at millimeter wavelength," *IEEE Trans. Microw. Theory and Techn.*, vol. 58, no. 12, pp. 3493–3501, Dec 2010.

[11] C. V. L.F. Chen, C.K. Ong and V. Varadan, "Chapter 5 - Resonator Methods," in *Microwave Electronics : Measurement and Materials Characterization*. Hoboken, UK: John Wiley & Sons, Incorporated, 2004.

[12] A. Penirschke, S. Muller, P. Scheele, C. Weil, M. Wittek, C. Hock, and R. Jakoby, "Cavity perturbation method for characterization of liquid crystals up to 35 GHz," in *34th Eur. Microw. Conf., 2004.*, vol. 2, Oct 2004, pp. 545–548.

[13] R. Kowerdziej, J. Krupka, E. Nowinowski-Kruszelnicki, M. Olifierczuk, and J. Parka, "Microwave complex permittivity of voltage-tunable nematic liquid crystals measured in high resistivity silicon transducers," *Applied Physics Letters*, vol. 102, no. 10, p. 102904, 2013. [Online]. Available: https://doi.org/10.1063/1.4795534

[14] R. Kowerdziej, J. Parka, J. Krupka, M. Olifierczuk, E. Nowinowski-Kruszelnicki, L. Jaroszewicz, and O. Chojnowska, "Dielectric properties of highly anisotropic nematic liquid crystals for tunable microwave components," *Applied Physics Letters*, vol. 103, no. 17, p. 172902, 2013. [Online]. Available: https://doi.org/10.1063/1.4826504

[15] M. Yazdanpanahi, S. Bulja, D. Mirshekar-Syahkal, R. James, S. E. Day, and F. A. Fernandez, "Measurement of dielectric constants of nematic liquid crystals at mm-wave frequencies using patch resonator," *IEEE Trans. Instrum. Meas.*, vol. 59, no. 12, pp. 3079–3085, Dec 2010.

[16] D. C. Zografopoulos, A. Ferraro, and R. Beccherelli, "Liquid-crystal high-frequency microwave technology: Materials and characterization," *Advanced Materials Technologies*, vol. 0, no. 0, p. 1800447, 2018. [Online]. Available: https://onlinelibrary.wiley.com/doi/abs/10.1002/admt.201800447

[17] J. Krupka, "Frequency domain complex permittivity measurements at microwave frequencies," *Measurement Science and Technology*, vol. 17, no. 6, pp. 55–70, April 2006.

[18] G. Kent, "Nondestructive permittivity measurement of substrates," *IEEE Trans. Instrum. Meas.*, vol. 45, no. 1, pp. 102–106, Feb 1996.

[19] M. D. Janezic and J. Baker-Jarvis, "Full-wave analysis of a split-cylinder resonator for nondestructive permittivity measurements," *IEEE Trans. Microw. Theory Techn.*, vol. 47, no. 10, pp. 2014–2020, Oct 1999.

[20] D. M. Pozar, *Microwave Engineering, 4th ed.* Hoboken, NJ, USA: John Wiley & Sons Inc., 2012.

[21] F. L. Penaranda-Foix and J. M. Catala-Civera, "Circuital analysis of cylindrical structures applied to the electromagnetic resolution of resonant cavities," in *Passive Microwave Components and Antennas*, V. Zhurbenko, Ed. Rijeka: IntechOpen, 2010, ch. 7. [Online]. Available: https://doi.org/10.5772/9400

[22] F. L. Penaranda-Foix, M. D. Janezic, J. M. Catala-Civera, and A. J. Canos, "Full-wave analysis of dielectric-loaded cylindrical waveguides and cavities using a new four-port ring network," *IEEE Trans. Microw. Theory Techn.*, vol. 60, no. 9, pp. 2730–2740, Sept 2012.

[23] D. Marques-Villarroya, F. L. Penaranda-Foix, B. Garcia-Banos, J. M. Catala-Civera, and J. D. Gutierrez-Cano, "Enhanced full-wave circuit analysis for modeling of a split cylinder resonator," *IEEE Trans. Microw. Theory Techn.*, vol. 65, no. 4, pp. 1191–1202, April 2017.

[24] J. Taylor, *An introduction to Error Analysis*. Sausalto, CA, USA: University Science Books, 1997.

Juan R. Sánchez received his MSc degree in Telecommunication Engineering from the Universitat Politécnica de Valéncia in 2014 (with first-class honors). In 2015 he received a MSc degree "Master Program in Electronics and Telecommunications" from Högskolan i Gävle, Sweden. In 2015 he gained a grant under the Fellowship Program for Training University Professors FPU14/00150 to get the PhD degree in Telecommunication, he is now working in the Microwave Application Group of the Institute of Telecommunications and Multimedia Applications of the Universitat Politécnica de Valéncia. His current research interests include analysis methods and computer aided design of passive microwave devices in waveguide and substrate integrated waveguide technologies.

Vicente Nova received his MSc degree in communication engineering from the Universitat Politécnica de Valéncia in 2016. He made his master's degree project on ESICL broadband transitions. His current research includes optimization and design of substrate integrated microwave devices, design and manufacture of SICs lines and design of reconfigurable devices using anisotropic materials.

Carmen Bachiller received her MSc degree in Telecommunication Engineering in 1996 and her PhD in Telecommunication in 2010 from the Universitat Politécnica de Valéncia. She worked from 1997 to 2001 in the ETRA I+D company as a project engineer in research and development on automatic traffic control, public transport management and public information systems using telecommunication technology. In 2001 she joined the Communication Department of the Universitat Politécnica de Valéncia as an assistant lecturer, she is an Associated Professor since 2011. She is teaching electromagnetism theory. She has participated in several teaching innovation projects and technological heritage studies. Her current research activities include modal methods for electromagnetic analysis, optimization and design of passive microwave structures, analysis and design of substrate integrated transmission lines and circuits and power effects in passive waveguide systems.

Belén Villacampa received her MSc degree in Physics in 1989 and her PhD in Physics in 1993 from the University of Zaragoza. She was granted a scholarship to carry out a postdoctoral stay at the "Centre National d'Études des Telecommunications" Bagneux-Paris. After her postdoc she joined the Department of Condensed Matter Physics of the University of Zaragoza, where she is Associate Professor, and the Institute of Material Science of Aragón. She is teaching General Physics and Optical and Spectroscopic Techniques. Her research activities have included the characterization of organic materials for nonlinear optical applications, having a focus on photoaddressable polymers showing liquid crystal phases. In recent years, her interest has expanded towards physical characterization of organic photovoltaic devices. She is co-author of 87 research articles. She has hold several management positions in the University, mainly related with doctoral training.

Alberto de la Rua received his diploma in Telecommunication Engineer in 2013 from the University of Alcala, Spain, and MSc degree in Communication Systems and Networks from the TH Cologne University of Applied Science in 2015. He made his master's degree project on methods for electrical characterization of materials at high frequencies, which has been continuously applied to new materials. In addition he works on small integrated antennas and his current research includes also new antenna measurement systems using unmanned aerial vehicles.

Rainer Kronberger (M'99) received Dipl.-Ing. degree in Electrical Engineering from the Technical University Munich in 1989 and the Dr.-Ing. degree from the University of the German Armed Forces, Munich, in 1996 about small array antennas for mobile communications. From 1999 until 2002 he was with Fuba Automotive / Delphi Automotive in Germany. In 2002 he changed to Infineon Technologies AG, Munich, where he was leader of the innovations group in the wireless division. End of 2004, he joined TH Cologne University of Applied Sciences, where he is currently full Professor at the Institute of Communications Engineering and head of the High Frequency Laboratory. His main field of research is in the area of antennas for mobile devices and vehicles, RFID technology, material measurements and microwave absorbers. He has authored or co-authored more than 100 publications and presentations in national and international conferences and journals and he contributed to more than 20 patents.

Felipe Peñaranda (M92-SM2015) was born in Benicarló (Spain) in 1967. He received the M.S. degree in electrical engineering from Universidad Politécnica de Madrid, Madrid, Spain, in 1992, and the Ph.D. degree in electrical engineering from Universidad Politécnica de Valencia (UPV), Valencia, Spain, in 2001. In 1992, he joined the Departamento de Comunicaciones, UPV, where he is currently a full professor. His current research interests include electromagnetic scattering, microwave circuits and cavities, sensors and microwave heating applications. He has co-authored more than 50 papers in referred journals, almost 100 papers in conference proceedings and more than 100 engineering reports for companies and public projects. In 2017 he has an h-index of 13, and i10 index of 19. Dr. Pearanda-Foix is IEEE and AMPERE member and reviewer of several international Journals.

Vicente E. Boria (S'91-A'99-SM'02-F18) was born in Valencia, Spain, on May 18, 1970. He received his Ingeniero de Telecomunicación degree (with first-class honors) and the Doctor Ingeniero de Telecomunicación degree from the Universidad Politécnica de Valencia, Valencia, Spain, in 1993 and 1997, respectively. In 1993 he joined the Departamento de Comunicaciones, Universidad Politécnica de Valencia, where he has been Full Professor since 2003. In 1995 and 1996, he was holding a Spanish Trainee position with the European Space Research and Technology Centre, European Space Agency (ESTEC-ESA), Noordwijk, The Netherlands, where he was involved in the area of EM analysis and design of passive waveguide devices. He has authored or co-authored 10 chapters in technical textbooks, 180 papers in refereed international technical journals, and over 200 papers in international conference proceedings. His current research interests are focused on the analysis and automated design of passive components, left-handed and periodic structures, as well as on the simulation and measurement of high power effects in passive waveguide systems. Prof. Boria has been a member of the IEEE Microwave Theory and Techniques Society (IEEE MTT-S) and the IEEE Antennas and Propagation Society (IEEE AP-S) since 1992. He acts as a regular reviewer of the most relevant IEEE and IET technical journals on his areas of interest. He has been Associate Editor of IEEE Microwave and Wireless Components Letters (2013-2018) and IET Electronics Letters (2015-2018). Presently, he serves as Subject Editor (Microwaves) of IET Electronics Letters, and as Editorial Board member of International Journal of RF and Microwave Computer-Aided Engineering. He is also member of the Technical Committees of the IEEE-MTT International Microwave Symposium and of the European Microwave Conference.